

An X-ray Image Recognition Model Based on Computer Image Recognition Ability

Servé W.M Weusthuis

Laboratory of Microbiology, Wageningen University & Research, the Netherlands

ABSTRACT

Pneumonia is an infection of the lungs caused by viruses, bacteria, etc. Pneumonia kills a large number of people every year. Timely diagnosis of pneumonia is the precondition of timely treatment. Chest X-rays have long been an important way to check for pneumonia. However, manual reading of X-ray images requires more time and is prone to misjudgment. But the pneumonia chest X-ray film, the characteristic is to have the very strong regularity, therefore uses the computer to carry on the accurate reading of the image, is a very desirable way. In this paper, an image recognition model is developed to identify pneumonia. In clinical practice, X-ray images can be better used to identify pneumonia as early as possible.

KEYWORDS

Chest X-ray; Object detection; Segmentation.

1. Introduction

X-ray image analysis is considered as tedious and crucial tasks for radiology experts. Therefore, researchers have proposed several computer algorithms to analyze X-ray images. Also, several computer assisted diagnosis tools [have been developed to provide an insight of X-ray images. However, these tools are not able to provide sufficient information to support doctors in making decisions. Machine learning is a promising approach in the field of artificial intelligence. A plenty of research works have been carried out to investigate the chest and lung diseases using machine learning. Vector quantization, regression neural networks has been used to investigate chest disease. In another study, chronic pneumonia disease was analyzed and its diagnosis was implemented using neural networks. Another study used chest radiographic images for the detection of lung diseases. They applied histogram equalization for image pre-processing and further feed forward neural network was used for classification. Although the above mentioned studies have performed efficiently, however lacks in terms of higher accuracy, computational time and error rate. Deep learning has already been proved an effective approach in object detection and segmentation, image classification, natural language processing etc. Further, deep learning has also shown its potential in medical image analysis for object detection and segmentation such as radiology image analysis in order to study anatomical or pathological structures of human body. Also, deep learning provided higher accuracy than traditional neural network architectures.

In the remainder of this article, we first review the literature related to pneumonia identification in chest X-ray images followed by proposed model architecture in Section 3 detailing algorithm and training steps in different stages. We have detailed our extensive analysis of RSNA dataset in Section 4 with image augmentation steps including the result from cleaned data, and evaluation metrics followed by evaluation result in Section 5 of our proposed model as well as ensembles of our model. Finally, we conclude our work in Section 6 along with future work.

2. Literature Survey

Roth et al. demonstrated the power of deep convolutional neural network (CNN) to detect the lymph node in clinical diagnostic task and obtained drastic results even in the presence of low contrast surrounding structures obtained from computer tomography. In another study, Shin et al. [1] addressed the problems of thoraco-abdominal lymph detection and interstitial lung disease classification using deep CNN. They developed different CNN architectures and obtained promising results with 85 percent sensitivity at three false positives per patient. Ronneburger et al. [2] developed a CNN approach with the use of data augmentation. They suggested that even trained on small samples of image data obtained from transmitted light microscopy; the developed model was able to capture high accuracy. Jamaludin et al. [16] applied CNN architecture to analyze the data obtained from spinal lumbar magnetic resonance imaging (MRI). They developed an efficient CNN model to generate radiological grading of spinal lumbar MRIs.

All these studies have performed well on radiological data except that the size of the data was restricted to few hundred samples of patients. Therefore, a detailed study is required to use the power of deep learning over thousand samples of patients to achieve the accurate and reliable predictions. Kallianos et al. presented a state of art review stating the importance of artificial intelligence in chest X-ray image classification and analysis. Wang et al. [18] addressed this issue and prepared a new database ChestX-ray8 with 108,948 front view X-ray images of 32,717 unique patients. Each of the X-ray images could have multiple labels. They used deep convolutional neural networks to validate the results on this data and obtained promising results. They mentioned that chestX-ray8 database can be extended by including more disease classes and would be useful for other research studies.

Rajpurkar et al. developed a 121 layer deep convolutional layer network chestX-ray14 dataset. This dataset is publically available with more than 0.1 million front view X-ray images with 14 disease labels. They mentioned that their algorithm is capable to predict all 14 disease categories with high efficiency. Irvin et al. [3] stated that large labeled dataset is the key to success for prediction and classification tasks. They presented a huge dataset that consists of 224,316 chest radiographic images of 65,240 patients. They named this dataset as CheXpert. Then they used convolutional neural networks to assign labels to them based on the probability assigned by model. Model used frontal and lateral radiographs to output the probabilities of each observation. Further, they released the dataset as a benchmark dataset. Besides the availability of a large dataset, it is highly desirable that every object in the image should be detected carefully and segmentation of each instance should be done precisely. Therefore, a different approach is required to handle both instance segmentation and object detection. Such powerful methods are faster region based CNN (F-RCNN) [4] and FCN (Fully Convolutional Network) [3].

Moreover, F-RCNN can be extended with an additional branch for segmentation mask prediction on each region of interest along with existing branches for classification task. This extended network is called Mask R-CNN and it is better than F-RCNN in terms of efficiency and accuracy. Kaiming He et al. [5] presented Mask R-CNN approach for object instance segmentation. They compared their results with best models from COCO

2016 [24,25]. Luc et al. [26] extended their approach by introducing an instance level segmentation by predicting convolutional features.

3. Experimental Evaluation

Dataset: We used a large publicly available chest radiographs dataset from RSNA which annotated 30,000 exams from the original 112,000 chest X-ray dataset [18] to identify instances of potential pneumonia as a training set and STR approximately generated consensus annotations for 4500 chest X-rays to be used as test data. The annotated collection contains participants ground truth which follows training our algorithm for evaluation. The sets containing 30,000 samples is actually made up of 15,000 samples with pneumonia related labels such as ‘Pneumonia’, ‘Consolidation’, and ‘Infiltration’, where 7500 samples are chosen randomly with ‘No Findings’ label, and another randomly selected 7500 samples without the pneumonia related labels and ‘No Findings’ label. They created a unique identifier for each of those 30,000 samples.

Annotation: Samples were annotated using a proprietary web based annotation system and permanently inaccessible to the other peoples’ annotations. Every radiologists practitioners who took part in training initially executed on the similar set of 50 exemplary chest X-rays in a hidden manner, and then were visibly annotated to the other practitioners for the similar 50 chest X-rays for evaluations, as it enable for questions such as does an X-ray with healed rib fractures enumerate and no enumeration as ‘Normal’ and for preliminary calibration. The final sets of label comprises of as given in Table 4: There are ‘Question’ labels to suggest questions which will be answered by a chest radiologist practitioner. Overall coequal distribution of 30,000 human lungs is annotated by six radiologists experts to assess whether the collected images of lungs opacities equivocal for pneumonia with their analogical bounding box to set forth the status. Also, other twelve experts from STR collaborated in annotating fairly 4500 human lungs. Out of 4500 triple read conditions, we divided these chest X-rays into three sets containing 1500 human lungs in training set, 1000 in test set (initial stage) and rest 2000 in test set at final stage. However, the test sets is double checked by five radiologist practitioners including six other radiologists from the first group.

Primary consideration: We discuss the adjudicate during the data collection for such sophisticated task. A bounding box is assessed as isolated in multi-read case provided that it does not coincide with the bounding boxes of the other two readers i.e., these two readers fails to flag that particular area of the image as being unsure for pneumonia. Whenever the adjudicator concurs that the isolated bounding box is valid then the box will endures a positive minority belief, in other cases it will be discarded. Initially, they assigned a confidence score to the bounding boxes. Also, a low confidence bounding boxes was discarded and high/ intermediate boxes was aggregated into a group of appropriate pneumonia. Given a low probability based bounding box, they discard the box and check whether the labeling is abnormal or no lung opacity. The opposed bounding boxes was adjudicated by one of two thoracic radiology practitioners in multi-read cases which does not consent. Also, the practitioners found that the annotations of all three readers in adjudicated case is more than 15%. They used intersection for the rest of the bounding boxes in case of at least 50% coincide by one of the bounding boxes, this step has ample effect in discarding few pixel data for multiple readers including positive pixels. They used 1500 read cases out of the 4500 triple cases into the training set to average out few probable distinction among single and multi-read cases. Rest 3000 triple read cases allocated to the test set. The majority vote is used to distinguish weak labels.

Table 1. RSNA training and test image set

# Images	Stage 1	Stage 2
Train Set	25684	26684
Test Set	1000	3000

Data augmentation: We performed augmentation on lung opacities and images data with random scaling including shifting in coordinate space $\delta x_1; y_1; \delta x_2; y_2$ as well as increasing/decreasing brightness and contrast including blurring with Gaussian blur under batches. Following these image augmentation, we found images after augmentation reported in Figure 1.

Considering the outcome in Figs. 2 and 3 signifies status of patient class and labels from the X-ray images, as we see a highly imbalanced dataset. The imbalance of training and test dataset among too many negatives and too few positives generates a critical issue, as we want high recall but the model could predict all negatives to attain high accuracy and the recall significantly undergo. In this case, it is unsure whether or not the present imbalance is acceptable or not. We test whether balancing the class distribution would yield any improvement in this case. To do this, we have trained our model on two training data sets, one balanced and the other not. We then create the balanced dataset by augmenting more images to the negative (0) class. We discussed previously the augmentation steps which includes flipping, rotating, scaling, cropping, translating, and noise adding. Introducing the images in the current negative class can possibly create radically new feature that does not exist in the other class. For example, if we choose to flip every negative-class image, then we have in the negative class a set of images that have the right and left parts of the bodies switched while the other class does not have this feature. This is not desirable because, the network may learn unnecessary (and incorrect) features such as the image with the left part of the body being to a certain side is more likely to exhibit non-pneumonia.

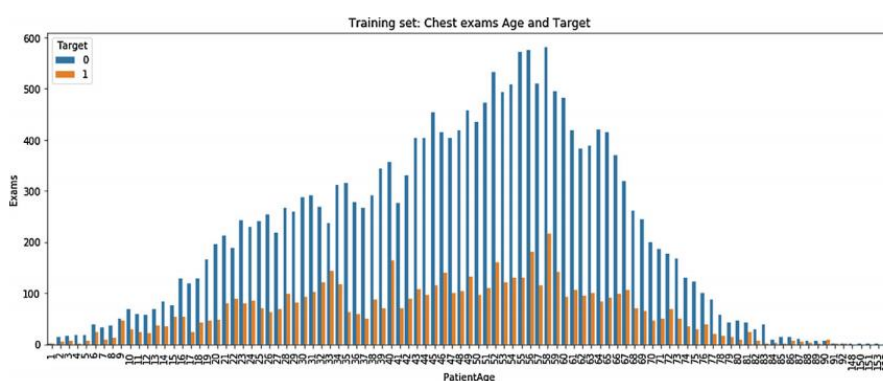


Figure 1. Positive and negative features among patients' of different age group.



Figure 2. Feature class of patients' among different age group

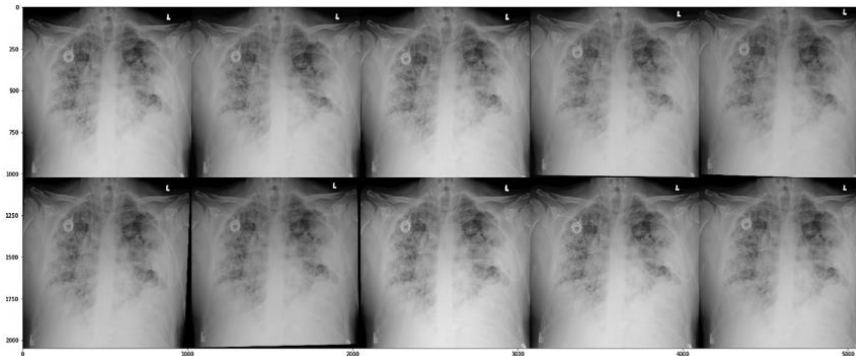


Figure 3. Augmentation on chest X-ray images.

We perform ensembling in Stage 2 due to labelled dataset, whereas the dataset in Stage 1 was highly imbalanced. The variance in the dataset is due to radiologists are overlooked with reading high volumes of images every shift. We have discussed this in earlier section of this article. In Figure 4, we overlay the probabilities of ground truth labels to check whether it is flipped or not. This also shows the successful predictions depicting inconsistency between ground-truth and prediction bounding boxes. We trained our proposed model in Stage 2 on NVIDIA Tesla P100 GPU and Tesla K80 in Stage 1, which also depicts that one needs an efficient computing resources to model such task on highly imbalanced dataset. The prediction outcome of our model at given threshold is reported in Table 6, in which the best prediction set of bounding boxes and ground-truth boxes results in Stage 2. Also, the predicted sample set depicting pneumonia showing the position

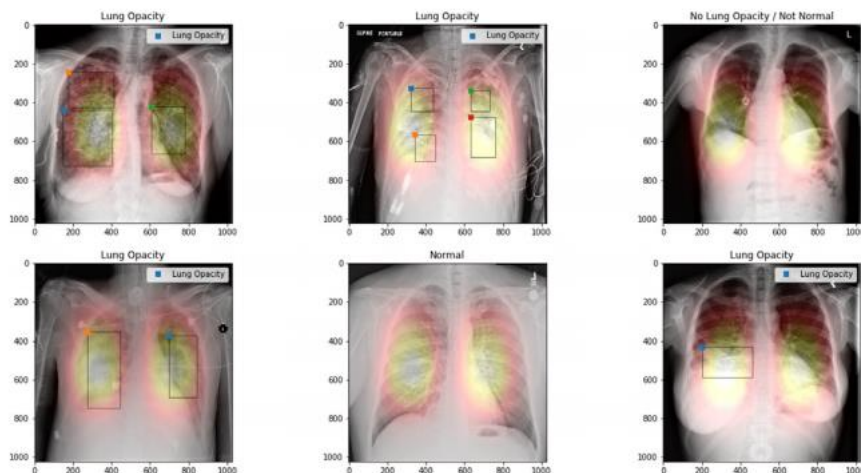


Figure 4. The results from stage 2 dataset.

4. Conclusion and Future Work

In this work, we have presented our approach for identifying pneumonia and understanding how the lung image size plays an important role for the model performance. We found that the distinction is quite subtle for images among presence or absence of pneumonia, large image can be more beneficial for deeper information. However, the computation cost also burden exponentially when dealing with large image. Our proposed architecture with regional context, such as Mask-RCNN, supplied extra context for generating accurate results. Also, using thresholds in background while training tuned our network to perform well in the this task. With the usage of image augmentation, dropout and L2 regularization prevented the overfitting, but are obtained something weaker results on the training set with respect to the test. Our model can be

improved by adding new layers, but this would introduce even more hyperparameters that should be adjusted. We intend to extend our model architecture in other areas of medical imaging with the usage of deep learning and computer vision techniques.

References

- U. Avni, H. Greenspan, E. Konen, M. Sharon, J. Goldberger, X-ray categorization and retrieval on the organ and pathology level, using patch-based visual words, *IEEE Trans. Med. Imaging* 30 (3), 2011, pp. 733-746.
- P. Pattrapisetwong, W. Chiracharit, Automatic lung segmentation in chest radiographs using shadow filter and multilevel thresholding, in: 2016 International Computer Science and Engineering Conference (ICSEC), IEEE, 2016, pp. 1-6.
- S. Katsuragawa, K. Doi, Computer-aided diagnosis in chest radiography, *Comput. Med. Imaging Graph.* 31 (4-5), 2007, pp. 212-223.
- Q. Li, R.M. Nishikawa, *Computer-aided Detection and Diagnosis in Medical Imaging*, Taylor & Francis, 2015.
- C. Qin, D. Yao, Y. Shi, Z. Song, Computer-aided detection in chest radiography based on artificial intelligence: a survey, *Biomed. Eng. Online* 17 (1), 2018, [20] p. 113.
- A.A. El-Solh, C.-B. Hsiao, S. Goodnough, J. Serghani, B.J. Grant, Predicting active pulmonary tuberculosis using an artificial neural network, *Chest* 116 (4) [21], 1999, pp. 968-973.
- O. Er, N. Yumusak, F. Temurtas, Chest diseases diagnosis using artificial neural networks, *Expert Syst. Appl.* 37 (12), 2010, pp. 7648-7655.
- O. Er, C. Sertkaya, F. Temurtas, A.C. Tanrikulu, A comparative study on chronic obstructive pulmonary and pneumonia diseases diagnosis using neural networks and artificial immune system, *J. Med. Syst.* 33 (6), 2009, pp. 485-492.

Copyrights

Copyright for this article is retained by the author(s), with first publication rights granted to the journal. This is an open-access article distributed under the terms and conditions of the Creative Commons Attribution license (<http://creativecommons.org/licenses/by/4.0/>).